UCRL-JC-122321
PREPRINT

Analysis of High Resolution Scatter Images from Laser Damage Experiments Performed on KDP

M. Runkel, B. Woods, M. Yan,
J. DeYoreo, and M. Kozlowski

This paper was prepared for submittal to
Symposium on Optical Materials for High Power Lasers
Orlando, Florida
October 30-November 1, 1995

January 5, 1996

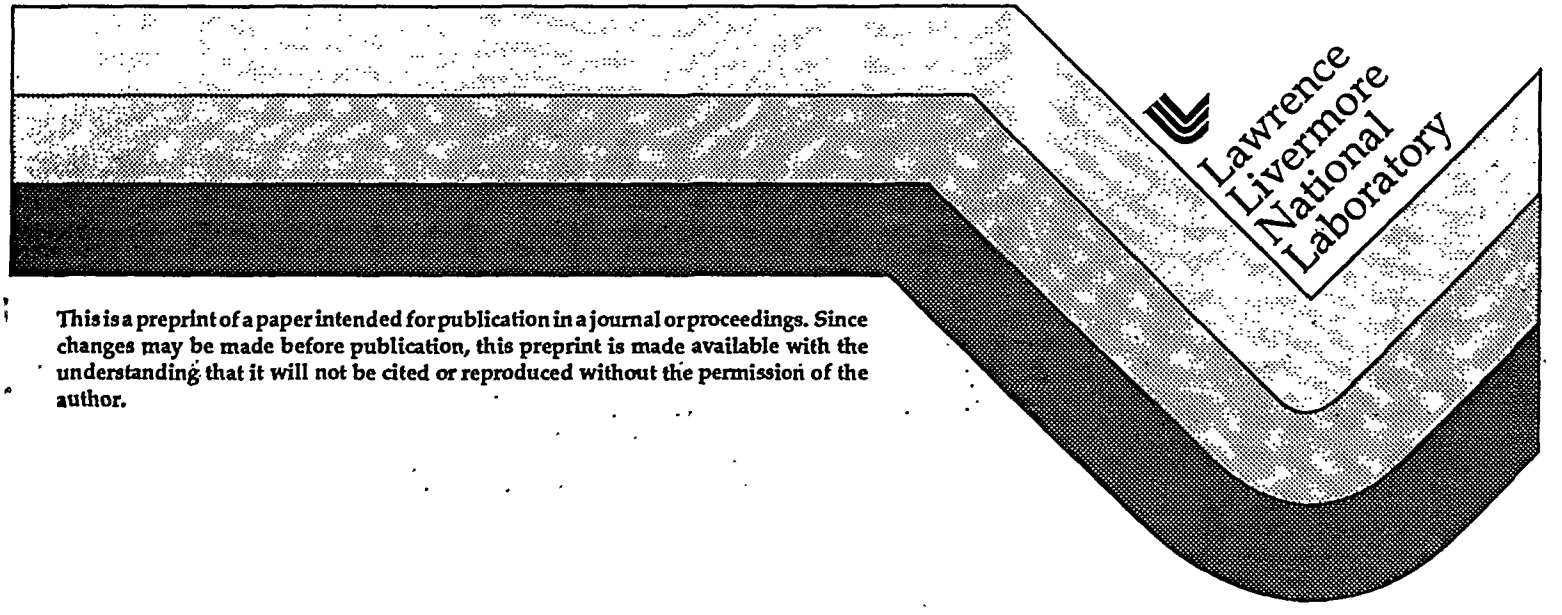

Analysis of high resolution scatter images from laser damage experiments performed on KDP

Mike Runkel, Bruce Woods, Ming Yan, Jim DeYoreo and Mark Kozlowski

Lawrence Livermore National Laboratory
P.O. Box 808, L-250
Livermore, CA 94550

ABSTRACT

Interest in producing high damage threshold KH_2PO_4 (KDP) and $(D_xH_{1-x})_2PO_4$ (KD*P, DKDP) for optical switching and frequency conversion applications is being driven by the system requirements for the National Ignition Facility (NIF) at Lawrence Livermore National Lab (LLNL). Historically, the path to achieving higher damage thresholds has been to improve the purity of crystal growth solutions. Application of advanced filtration technology has increased the damage threshold, but gives little insight into the actual mechanisms of laser damage. We have developed a laser scatter diagnostic to better study bulk defects and laser damage mechanisms in KDP and KD*P crystals. This diagnostic consists of a cavity doubled, kilohertz class, Nd:YLF laser (527 nm) and high dynamic range CCD camera which allows imaging of bulk scatter signals. With it, we have performed damage tests at 355 nm on four different "vintages" of KDP crystals, concentrating on crystals produced via fast growth methods. We compare the diagnostic's resolution to LLNL's standard damage detection method of 100X darkfield microscopy and discuss its impact on damage threshold determination. We have observed the disappearance of scatter sites upon exposure to subthreshold irradiation. In contrast, we have seen scatterers appear where none previqusly existed. This includes isolated, large (high signal) sites as well as multiple small scatter sites which appear at fluences above 7 J/cm^2 (fine tracking). However, we have not observed a strong correlation of preexisting scatter sites and laser damage sites. We speculate on the connection between the laser-induced disappearance of scatter sites and the observed increase in damage threshold with laser conditioning.

1. INTRODUCTION

KDP and KD*P are used in optical switching and frequency doubling and tripling applications in inertial confinement fusion (ICF) laser systems at LLNL (NOVA, Beamlet, NIF). Each successive generation of ICF laser system has increased the laser damage requirements of the crystals used in it. There have been numerous techniques developed to purify growth solutions[1,2,3] which have resulted in crystals with higher damage thresholds. LLNL has compiled an extensive database on the laser damage performance of KDP and KD*P which bears this out[4]. Figure 1 shows a plot of conditioned and unconditioned bulk damage thresholds as a function of year grown for all crystals tested at 1064 nm (1ω) and 355 nm (3ω) at LLNL. The trend toward higher thresholds at both wavelengths is clear in spite of the large scatter in the data.

As shown in Table 1, KDP crystals produced by state-of-the-art conventional (slow growth) technologies have nominal unconditioned (S:1) and conditioned (R:1) thresholds which exceed NIF requirements. Despite this, there are still many unresolved laser damage issues which merit attention. Note that KD*P, used for frequency tripling, does not now meet NIF requirements unless thresholds are raised by laser conditioning - currently a process which is not well understood. In addition, production requirements for the NIF demand approximately 600, 30 cm crystals of high optical quality. With current conventional growth techniques, approximately two years are required to grow a KDP boule which will meet NIF size requirements. Application of fast growth techniques has exhibited an approximate tenfold increase in the rate of crystal growth[5,6] over conventional growth methods. The potential time and cost savings resulting from producing these crystals by fast growth methods is enormous. Currently, however, the laser damage thresholds of fast grown KDP and KD*P do not meet NIF requirements or compare with the best conventionally grown crystals.

Table 1. Nominal laser damage thresholds of conventional crystals and NIF design requirements for KDP and KD*P at 3 ns.

Function, material, wavelength	Damage threshold (J/cm2)		NIF requirements
	S:1	R:1	
Optical switch, KDP, 1064 nm	30	40	14.9
Frequency doubler, KDP, 1064 nm	30	40	15
Frequency tripler, KD*P, 355 nm	10	20	12.7

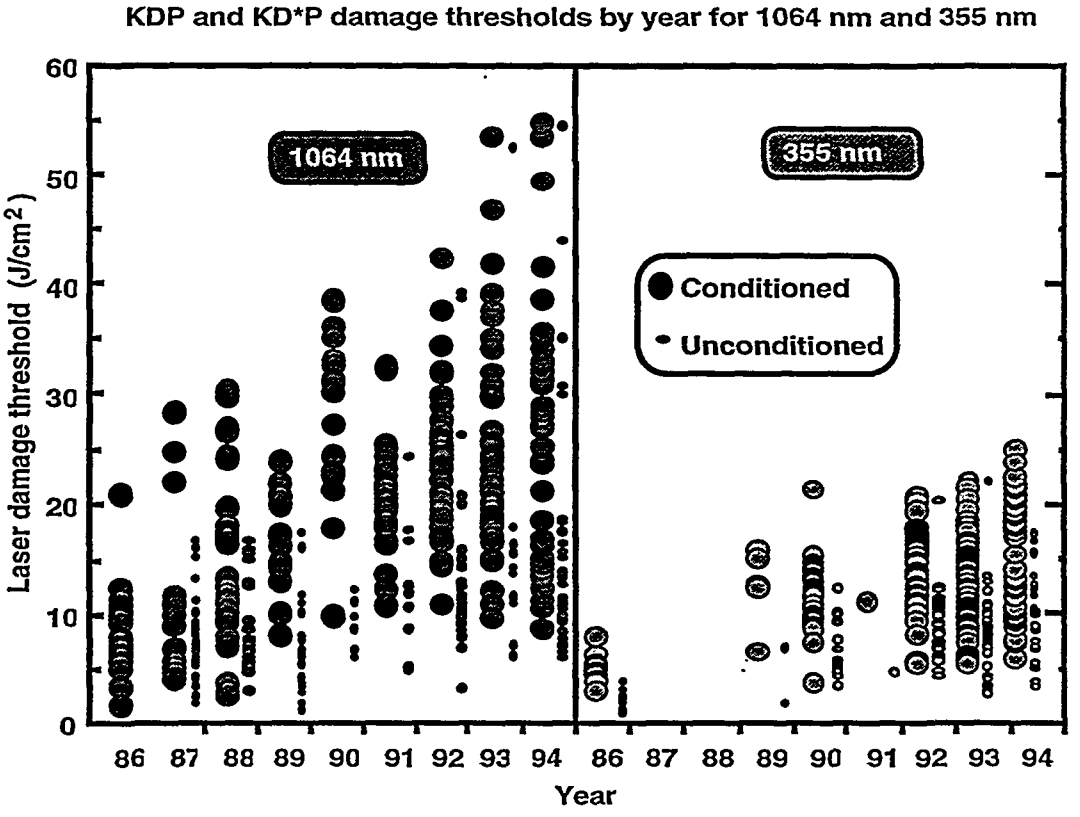

Figure 1. Increase in the laser damage threshold of KDP and KD*P by year for testing at 1064 nm and 355 nm. $\tau^{0.5}$ scaling has been used for data of various pulse lengths to calculate equivalent thresholds for 3 ns pulses. Data courtesy of Frank Rainer, LLNL, reference 7.

2. TEST APPARATUS AND SCATTER MEASUREMENT

2.1 Test apparatus and samples

The apparatus we used to obtain bulk scatter images is shown below in figure 2. The probe beam was provided by a cavity doubled Nd:YLF laser (527 nm) operating at 4.0 kilohertz. The laser's power output was 165 mW in a gaussian beam of 1.6 mm ($FW1/e^2$). The irradiance on the sample was approximately 15 W/cm^2, which was sufficient to induce Rayleigh scatter and fluorescence in the test samples. The probe laser was also linearly polarized and equipped with a rotatable halfwaveplate to control the polarization incident on the sample. We imaged light scattered out the side of the sample at 90 degrees by using a 14 bit, 1024 X 1024, 20 micron pixel CCD array in conjunction with a f = 135 mm camera lens and bellows attachment. The overall system magnification was approximately 2X. For these tests the incident angle was normal to the crystal face and the view angle fixed at 90 degrees. Images were captured and stored on computer using software supplied with the CCD camera. We were able to select the field of view to eliminate unwanted camera saturation effects from surface scatter. The system software also allowed us to control the overall exposure via shutter speed control. Exposures as low as 10 ms were possible. In addition to damage testing, we have used the diagnostic to investigate other features such as variations in growth planes in KDP[8]. We are currently assessing the impact of these growth plane variations on damage processes in KDP.

We mounted the scatter diagnostic onto the ZEUS damage test facility. The ZEUS facility consists of a 10 Hz, Nd:YAG laser capable of 100 J/cm^2 in an 8 ns pulse at 1064 nm and 50 J/cm^2 in a 7.5 ns pulse at 355 nm. The nominal spot used was

1.0 mm ($FW1/e^2$). All the tests described here were performed at 355 nm. We performed microscopic inspections by rotating the sample under test 90 degrees up to the Nomarski/darkfield microscope. The sample was illuminated from behind via a white light source delivered by optical fiber bundle. Prior to testing, we established damage and probe beam alignment using a dummy sample and video camera. We could align the two beams with a peak-to-peak separation of less than 250 microns this way. We were able to refine and maintain probe and damage beam alignment during testing by centering the Rayleigh component of the scatter signal on a damage track from a previous test site.

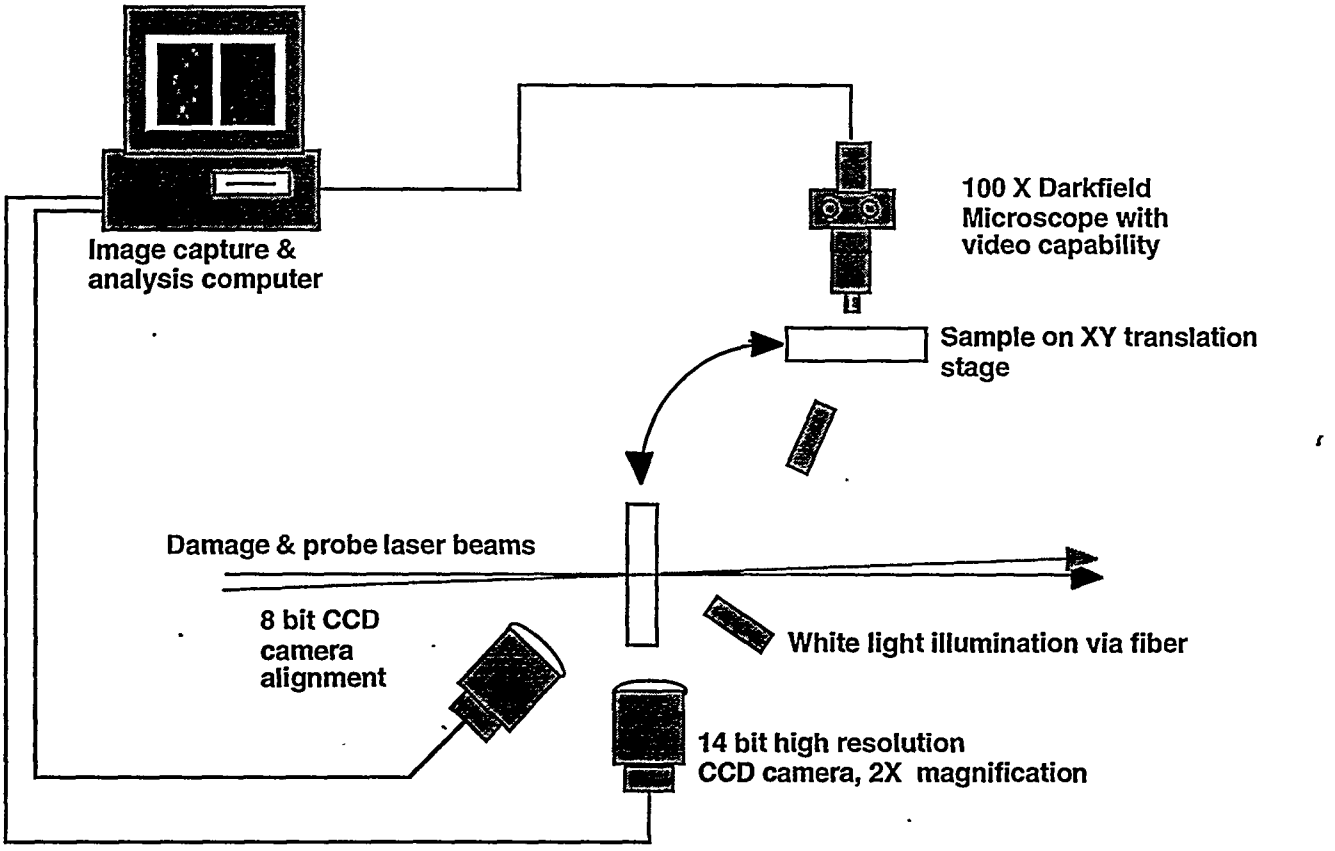

Figure 2. Schematic of microscopy and scatter diagnostic apparatus .

The samples we tested typically had dimensions of 10 cm X 10 cm X 1 cm and were diamond turned on the front and rear surfaces. Imaging the bulk scatter signal was facilitated with the aid of a good surface polish on the sides of the test samples. The samples were z-plates and thus incapable of harmonic generation. Additionally, z cut crystals are highly symmetric about the crystals z axis and allow examination of prism and pyramid sectors. Figure 3 shows the major components of a fast grown KDP boule including the prism and pyramid sectors and the region from which a z-plate is taken.

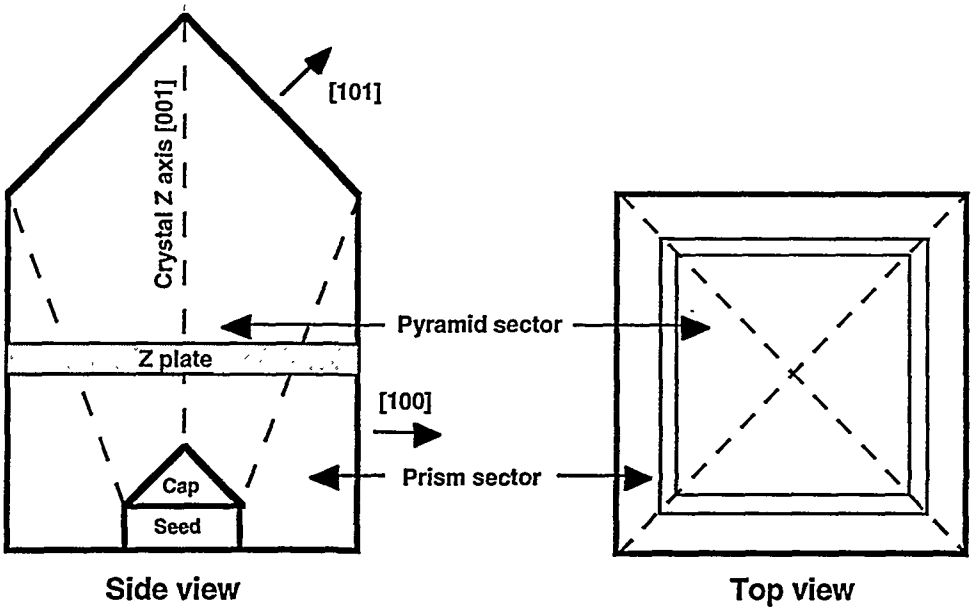

Figure 3. Schematic side view of fast grown KDP boule and top view of a z-cut plate. The pyramid sector is within the central portion of the boule while the prism sector lies outside. A z-plate is cut perpendicular to the crystal's z axis. It is ideal for damage testing because it does not cause harmonic generation and can contain portions of both prism and pyramid sectors. (Reference 5.)

2.2 Components of scatter

The scatter signal we observed consisted of several components as shown in figure 3. The features of greatest interest in this work were the large scale discrete (Mie) scatter points. These occurred in widely varying density depending on the vintage of crystal under test. The Rayleigh and fluorescence components are also present in the scatter images. They provide a background signal which corresponds to the width of the probe beam in the sample. As expected, the Rayleigh signal showed a strong dependence on the probe laser polarization (horizontal or vertical) relative to the view angle. The waveplate was set to 45 degrees between horizontal and vertical polarization during testing.

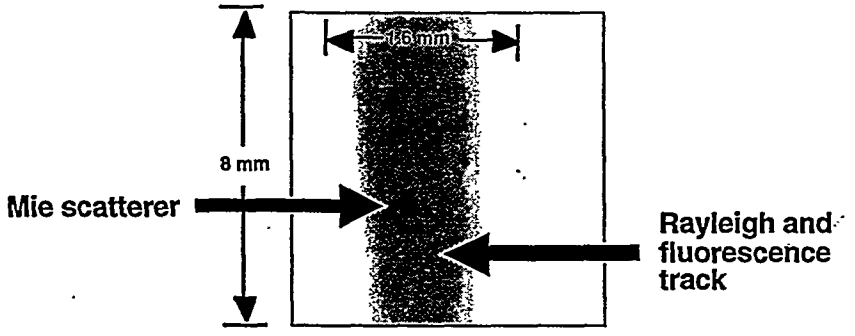

Figure 3. Scatter image in inverted gray scale showing bulk Mie scatterers as dark spots. The Rayleigh and fluorescence track appears as the lighter, wide gray image.

2.3 Number density of crystal vintages

Prior to damage testing we examined a number of crystals from different chronological "vintages" related to the construction of various ICF laser systems at LLNL. In particular the crystals were examined for number density of Mie scatterers. The

crystals we tested included conventional growth examples prior to 1987 without any solution filtration (NOVA prefiltration), those grown between 1987 and 1990 during the development of solution filtration techniques (NOVA postfiltration), the best conventionally grown crystals currently available (Beamlet), as well as current LLNL fast grown crystals with no filtration. The results listed in table 2 show the crystal vintage, the average number of scatterers associated with it, and the median and maximum damage thresholds taken from the database at 1ω and 3ω.

Table 2. Average number of Mie scatters for each crystal vintage and its associated median and maximum unconditioned, S:1, and conditioned, R:1 damage thresholds at 1ω and 3ω for 3 ns pulses at 10 Hz.

Crystal Vintage	Average number of Mie scatterers (N/cm^3)	1ω damage threshold data (J/cm^2)				3ω damage threshold data (J/cm^2)			
		Median		Maximum		Median		Maximum	
		S:1	R:1	S:1	R:1	S:1	R:1	S:1	R:1
Nova prefiltration (1986)	1700	10.7	17.2	15.6	24.8	8.1	12.7	11.0	19.5
Nova postfiltration (1987 - 1990)	20	12.4	26.1	15.7	35.1	9.5	15.4	13.3	19.6
Beamlet (1994)	< 5	35.1	41.5	>54	>54	14.1	20.6	>23	>25
Fast grown (1995)	185	9.4	14.0	10.1	16.3	6.6	10.1	10.6	13.3

3. DAMAGE TESTING

3.1 Test procedure

We characterized intrinsic crystal defects and laser -induced damage sites using both standard optical microscopy techniques and the new scatter diagnostic. The LLNL standard unconditioned S:1 test procedure and inspection criteria were used in this work. The procedure consisted of a preexposure scan through the bulk of the material with 100X magnification and backlighting to produce darkfield illumination. We noted preexisting scatter sites and then exposed the site to 600 pulses (60 seconds) of fixed fluence irradiation and then reinspected it. We defined damage as any observable change in the material attributable to laser irradiation which was visible under 100X magnification. We then recorded images of the damage sites using the optical microscope for comparison of size and correlation to damage sites appearing in the scatter images. Damage generally appeared as pinpoints as small as 5 microns. Pre- and post-exposure scatter images of the test site were also recorded. This procedure was repeated on a virgin sites until enough data had been accumulated to determine a damage threshold. It was calculated as the average value between the lowest fluence damage site and the first non-damaging site at lower fluence. The fluence measurement precision was ±15%.

In addition, it was also our goal to investigate differences in damage threshold between prism and pyramidal crystal sectors, so individual damage tests were performed in each of these area on both crystals. Prior to testing the crystals had been mapped for UV absorption in the 200 nm and 300 nm bands as well as for stress birefringence in both prism and pyramidal sectors. Results of testing as related to UV absorption in the material were discussed in another paper at this symposium[15].

3.2 Standard test results and general observations

Table 3 shows the damage thresholds resulting from standard inspection techniques in samples 5-3 and 51-1-2 for the prism and pyramid sectors.

Table 3. Damage threshold results from standard 100X darkfield microscopic inspection techniques.

Sample	Prism threshold (J/cm^2)	Pyramid threshold(J/cm^2)
5-3	8.0 ± 1.2	6.2 ± 1.0
51-1-2	6.1 ± 0.9	5.8 ± 0.9

Initial optical microscopic inspections of the crystals showed very few preexisting defects (pinpoints) at the test sites. After we exposed the sites at threshold fluences, pinpoint damage of low number density (<5 pinpoints/test site) was observed. In

comparing the microscope to the scatter diagnostic it was immediately apparent that with the scatter diagnostic we could detect events beyond the capability of the darkfield microscope. We did not observe a strong correlation between the two diagnostics for preexisting scatter sites or sites which formed at near threshold fluences. Also, because the scatter diagnostic is more sensitive, we observed "subthreshold" site formation with it which we could not see with the microscope. We observed good correlation between the two diagnostics only at higher fluences when damage increased in severity. Two additional effects which we could observe with the scatter diagnostic but not the microscope were the disappearance of a high percentage of preexisting sites at all exposure fluences used in testing, even as low as 2.8 J/cm^2. This effect is shown in Figure 4. We also consistently observed the formation of numerous, small scatter sites upon exposure of the samples to fluences above 7 J/cm^2. In addition, we noted damage (i.e. large scatter signals) occurring at some preexisting scatter sites. This occurred with much lower frequency, however, than the formation of damage in regions where scatter sites previously were not visible. Examples of "fine tracking" and preexisting scatter site damage are shown in figure 5. By capturing sequences of images taken during testing we ascertained that in most instances the appearance or disappearance of scatter sites occurred after the first laser pulse. Once a site either appeared or disappeared it did not change on subsequent shots.

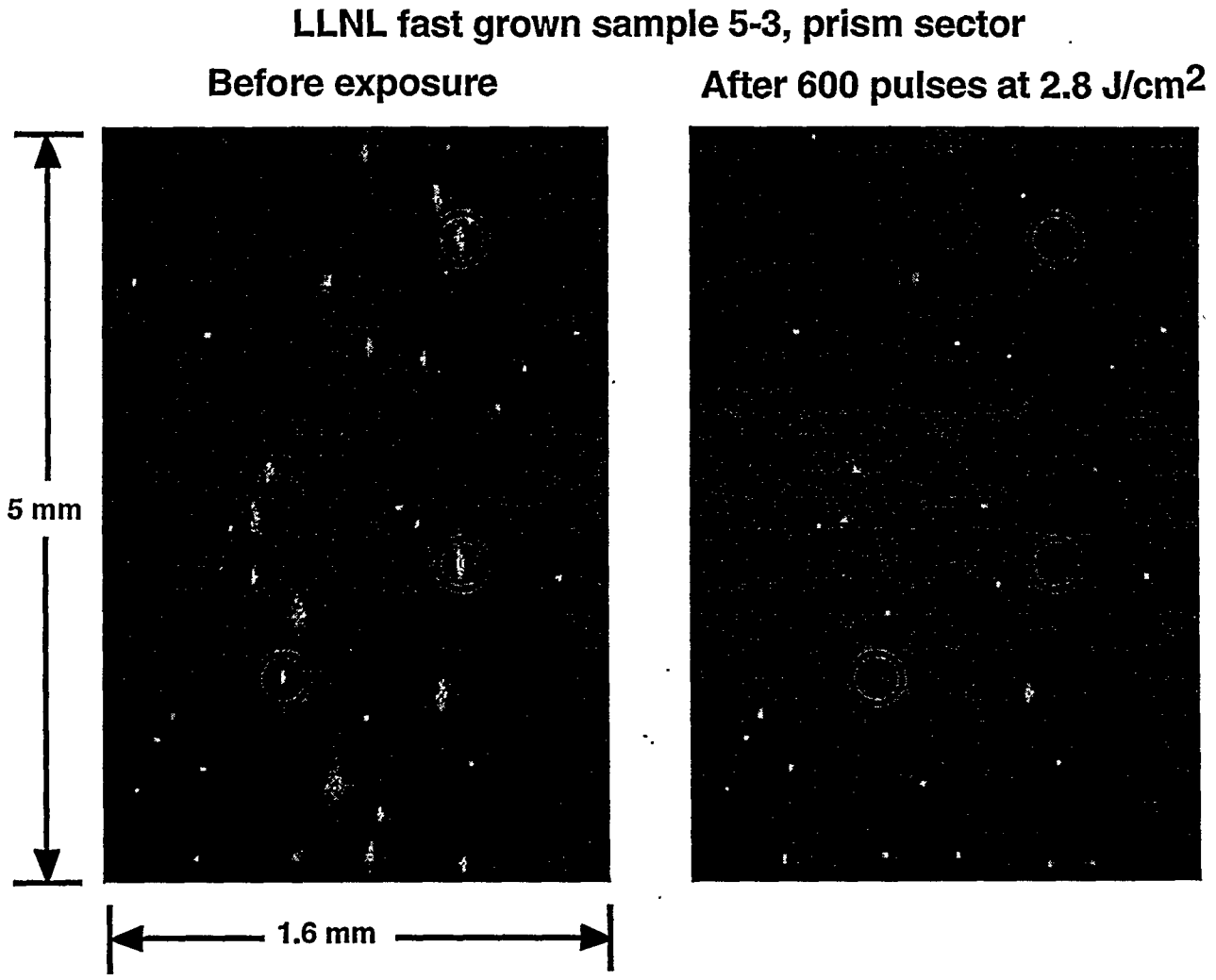

Figure 4. Before and after scatter images of the prism sector of sample 5-3 illustrating the disappearance of Mie scatterers when exposed to subthreshold fluences during S:1 testing. The circles in each image indicate sites which have disappeared completely while other sites show dramatic reduction in intensity. The measured damage threshold for the prism sector of this sample was 8.0 J/cm^2.

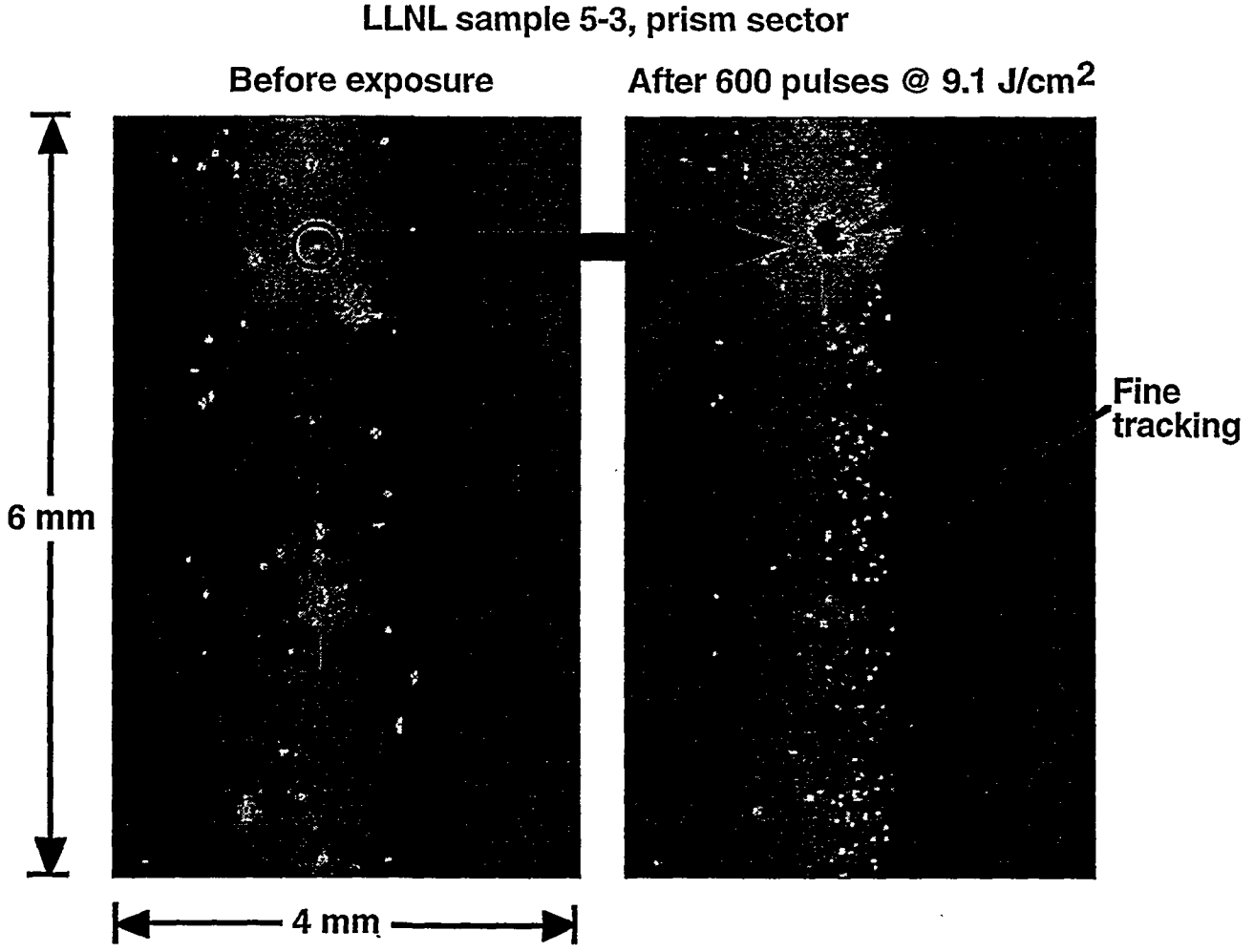

Figure 5. Before and after exposure scatter images of a test site in the prism sector of sample 5-3. The images illustrate the removal (conditioning) of scatter sites upon laser exposure as well as the formation of large scatter sites at a preexisting site (indicated by the circle), and fine tracking. The site was exposed to 600 pulses at an average fluence of 9.1 J/cm^2.

3.3 New scatter site generation and disappearance probabilities

We analyzed the scatter images do determine the initial number of scatterers and the number which appeared or disappeared due to laser exposure. For this work we sought to perform the most straightforward analysis possible, which was to count scatter sites. To facilitate this rather tedious chore, we developed image analysis programs using ConceptVI[9] subroutines and the LABVIEW[10] programming language. Once we had analyzed the images, the data was plotted to show trends in disappearance probability and new site generation as a function of exposure fluence. We defined the disappearance probability as the percentage of total sites which vanished due to laser exposure. Data plots of disappearance probability and new site generation for the prism sectors the two test samples are shown in figures 6 and 7. We have not shown data for the pyramidal sectors as it does not differ statistically from the prism sector. The average disappearance probability for sample 51-1-2 is 35%. In contrast, the average disappearance probability for sample 5-3 is 60%. We see no correlation to the exposure fluence in either plot.

Initial data on the number of sites created versus fluence suggests that the site generation rate is higher above the microscope-determined damage threshold and that the generation rate may be higher for sample 51-1-2 than for sample 5-3. We require

further data to verify the trends. In future testing, we will also analyze data for changes in signal magnitude in addition to counting statistics.

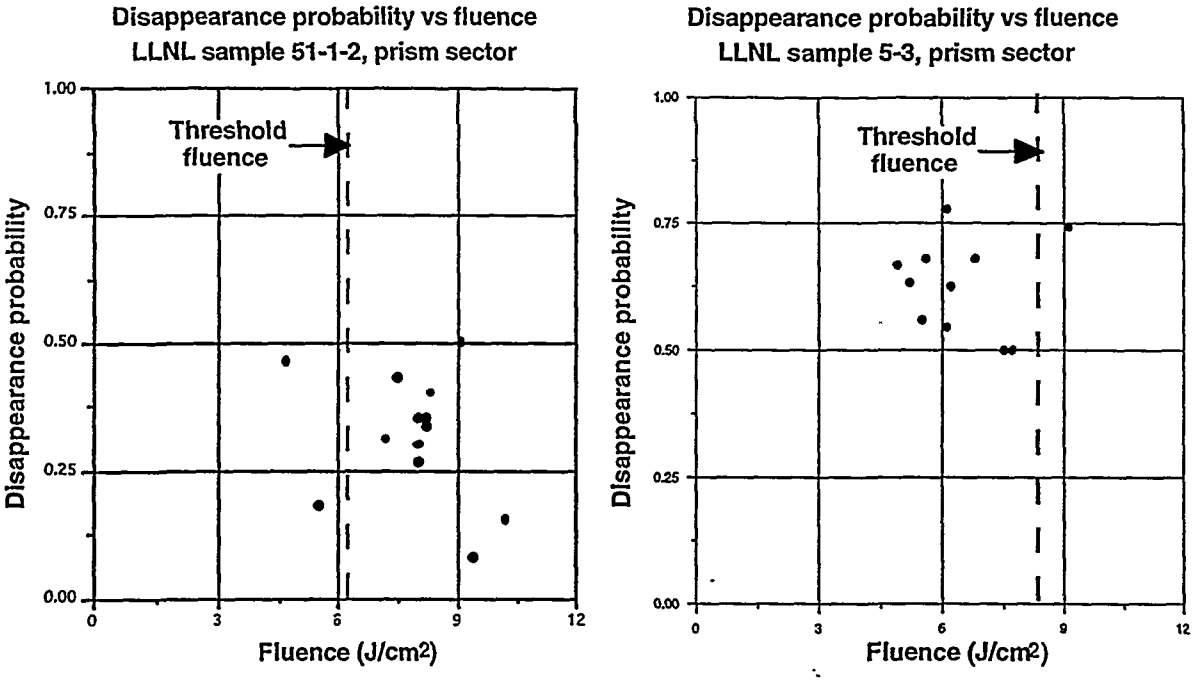

Figure 6. Disappearance probabilities for the prism sector of samples 51-1-2 and 5-3. The two samples show significant differences with average disappearance probabilities of 35% and 60% respectively. There does not seem to be a trend as a function of exposure fluence.

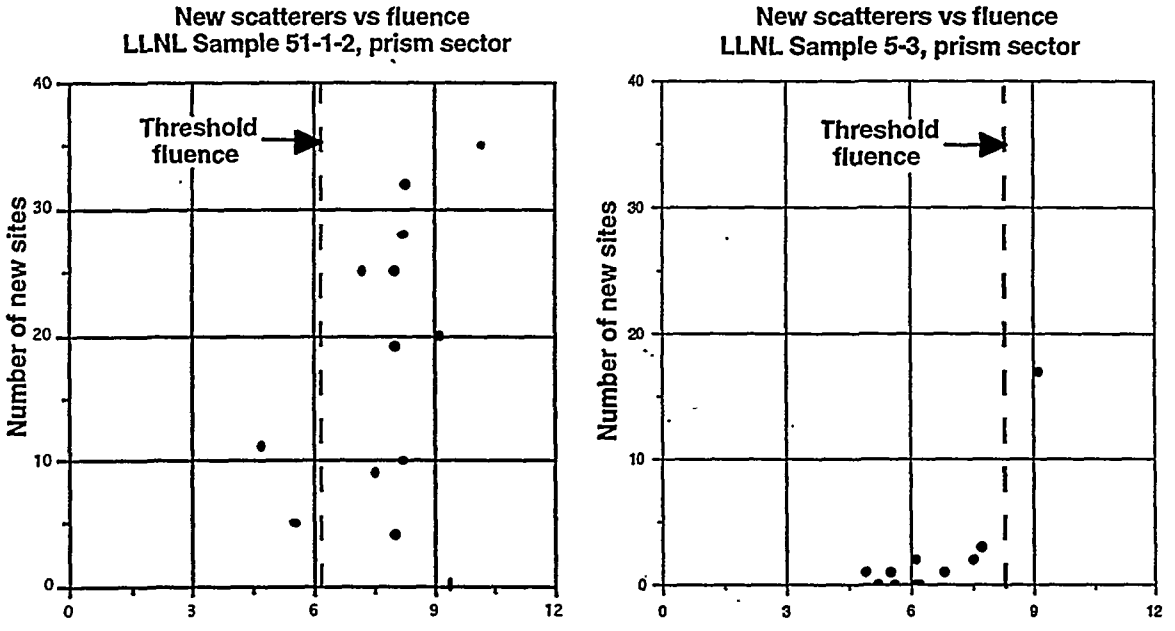

Figure 7. The production of new scatter sites for the prism sector of samples 51-1-2 and 5-3. The two samples again show significant differences in behavior. Note, however, that the two samples should not be compared as the majority of data in 51-1-2 was taken above threshold while for sample 5-3 it was taken below threshold.

4. DISCUSSION

We have observed significant new effects using the scatter diagnostic. In this section we speculate on possible explanations for the scatter sites and observed laser interactions with these, and consider the impact of these findings on LLNL's standard damage testing procedures.

4.1 Possible mechanisms

Our leading hypotheses regarding the nature of the Mie scatterers is that they are liquid or gas filled inclusions nucleated by microcontaminants. Such inclusions have been observed in KDP crystals during growth and can have sizes on the micron scale [13]. This would make them easily visible with our scatter diagnostic. The inclusions may be sites of laser damage because of local electric field enhancement, high stresses, or high absorption due to the microcontaminant or structural defects. We are currently applying several techniques to better ascertain the nature of the Mie scatterers. We have applied the Becke line test [14] and believe that the refractive index of the scatter sites is lower than that for the surrounding KDP crystal, consistent with the gas/liquid filled inclusion hypotheses. We have yet to determine an index value however. We also have an effort underway to investigate the scatter sites by fracturing through the damage tracks. This approach allows the defects to be probed for nucleating contaminants using well established surface analysis techniques. Chemical and spectroscopic analysis on the crystals and solutions from which they are grown are also being performed in an effort to understand the nature of the contaminants and how they are incorporated into the crystal lattice.

A likely explanation for the appearance or disappearance of scatter sites upon laser irradiation is laser-induced shape changes of the Mie scatterers. It has been shown for other crystal systems [11,12] that defects can be strongly faceted. This is likely the case for KDP as well. The faces could act as specular reflectors (mirrors) and scatter light in a highly directional manner. If this were the case, only slight changes in the shape of the scatter site would be necessary to redirect the scattered light into or out of the diagnostic's field of view, thereby accounting for the appearance or disappearance of scatter sites. We speculate that the laser pulse can upset the equilibrium state of the inclusion and cause the trapped supersaturated solution to crystallize, which either heals the inclusion completely or at least reduces it to a size below the resolution limit of the scatter diagnostic. To test this model, we studied the change in scatter intensity as a function of viewing angle. Preliminary results indicate that while the intensity of Mie scatterers changes with viewing angle they do not become undetectable by the scatter diagnostic. This suggests that while shape changes play a role, Mie scatter sites may actually be created and destroyed by the illumination process. If laser damage does initiate at the scatter points then this healing process can be the mechanism for laser conditioning.

4.2 Impact on standard damage test methods

100X Nomarski/darkfield microscopy has been used as the standard damage diagnostic for over fifteen years at LLNL. The new scatter diagnostic has been shown, however, to be more sensitive to laser-induced changes in the KDP crystals. We have concluded that the thresholds obtained using 100X microscopy are conservative enough to provide a good margin of safety for design specifications of ICF class lasers such as the NIF. Consequently this technique will remain LLNL's standard for the foreseeable future. For the purposes of studying laser damage and conditioning mechanisms the increased sensitivity of the scatter diagnostic is advantageous. We are therefore examining upgrading the standard optical microscope's performance by increasing the illumination intensity on the sample. Currently, the intensity is approximately 20 mW/cm^2. We expect that much more detail would be revealed if the illumination intensity were raised to that of the scatter diagnostic (15 W/cm^2). The short depth of focus of the microscope would offer the additional advantage of being able to map the crystal in three dimensions, a process that would be difficult with present scatter diagnostic.

5. CONCLUSION

We have developed a diagnostic system for imaging bulk scatter sites in KDP. With this diagnostic, we have performed damage tests on fast grown crystals. We have observed previously unseen effects in KDP including the disappearance of significant numbers of scatter sites upon laser irradiation, even at subthreshold fluences, the appearance of scatter sites in virgin material, the appearance of fine tracking in fast grown crystals above 7 J/cm^2 and the appearance of some laser damage at preexisting defects. We have performed experiments to investigate changes in scatter site intensity as a function of view angle and found that the scatter sites remain detectable at all angles, although the scattered light intensity may vary considerably. We have been able to determine that the Mie scatterers index of refraction is less than the surrounding crystal. We have speculated that the interaction of liquid filled inclusions with the laser accounts for the observed phenomena.

This work was performed under the auspices of the U.S. Department of Energy by Lawrence Livermore National Laboratory under Contract No.W-7405-ENG-48.

6. REFERENCES

1. K.E. Montgomery and F.P Milanovich, "High laser damage threshold potassium dihydrogen phosphate crystals," Journal of Applied Physics, **68**(8), 3979 - 3982, 1990.

2. A. Yokotani, T. Sasaki, K. Yoshida, T Yamanaka and C. Yamanaka, "Improvement of the bulk laser damage threshold of potassium dihydrogen phosphate crystals by ultraviolet radiation," in Laser Induced Damage in Optical Materials, National Bureau of Standards Special Publication **746**, edited by H.E. Bennet et. al., 101-107, 1985.

3. A. Yokotani, T. Sasaki, K. Yoshida, T. Yamanaka, S. Nakai and C. Yamanaka, "Effect of residual organic carbon in mother solution of potassium dihydrogen phosphate on damage threshold of the crystals for high power lasers, " in Laser Induced Damage in Optical Materials, National Institute of Standards and Technology Special Publication **775**, edited by H.E. Bennet et. al., 35 - 40, 1988.

4. F. Rainer, L.J. Atherton, J. J. DeYoreo, "Laser damage to production- and research-grade KDP crystals," in Laser Induced Damage in Optical Materials, SPIE Proceedings, Volume **1848**, edited by H.E. Bennet et. al., 46 - 58, SPIE, Bellingham, WA 1992.

5. J.J. DeYoreo et. al., "Development of large aperture KDP crystals," ICF Quarterly Report, 3(3), 103 - 111, Lawrence Livermore National Lab, Livermore, CA, UCRL-LR-105821-93-3 1993.

6. N.P. Zaitseva, I.L. Smol'skii and L.N. Rashkovich, "Study of rapid growth of KDP crystals by temperature lowering," Soviet Journal of Crystallography , *36*, 113 1991.

7. F. Rainer et. al., "A historical perspective on fifteen years of laser damage thresholds at LLNL," in Laser Induced Damage in Optical Materials, , SPIE Proceedings, Volume **2114**, edited by H.E. Bennet et. al., 9-22, SPIE, Bellingham, WA 1993. Data has been updated to include tests performed in 1994.

8. B. Woods, M. Runkel, M. Yan, J.J. DeYoreo and M. Kozlowski, "Optical scatter as a diagnostic tool for studying bulk defects which cause laser damage in conventional and rapid growth KDP and DKDP," in Optical Scattering in the Optics, Semiconductor, and Computer Disk Industries, , SPIE Proceedings, Volume **2541**, edited by J.C. Stover, SPIE, Bellingham, WA 1995.

9. Concept VI, Le moulin de l'image, 26270 MIRMANDE, France

10. LabVIEW, version 3.1, National Instruments Corporation, 6504 Bridgepoint Parkway, Austin, TX 78730

11, T.R. Anthony and H.E. Cline, "Thermal migration of liquid droplets through solids," Journal of Applied Physics, **42**(9), 3380 - 3387, 1971

12. D.R. Olander, A.J. Machiels, M. Balooch and S.K. Yagnik, "Thermal gradient migration of brine inclusions in synthetic alkali halide single crystals," Journal of Applied Physics, 53(1), 669 - 681, 1982

13. I. Smol'skii., J.J De Yoreo, J.D. Lee, T.A. Land and E.B Rudneva, "Oriented liquid inclusions in KDP crystals," Journal of Crystal Growth (in review).

14. D. McKie, C. McKie, Crystalline Solids, 400 - 402, John Wiley & Sons, New York, 1974

15. M. Yan, J.J. DeYoreo, N. Zaitseva and R. Torres, "Impurity contamination in fast grown KDP," presented at 1995 Boulder Damage Symposium. Paper not submitted.